

## Multiple muons in the Utah detector. II. Comparison with a hadronic scaling model\*

J. W. Elbert, J. W. Keuffel,<sup>†</sup> G. H. Lowe, and J. L. Morrison  
*Department of Physics, University of Utah, Salt Lake City, Utah 84112*

G. W. Mason  
*Department of Physics, Brigham Young University, Provo, Utah 84602*  
 (Received 18 February 1975)

Detailed predictions are made for the multiple-muon-event rates measured in the underground muon experiment at the University of Utah. In our calculations, Feynman scaling is used to project inclusive proton-nucleus particle production cross sections from 19.2-GeV accelerator measurements to the ultrahigh-energy region from 1 TeV to 10000 TeV. The multiplicity distribution is assumed to follow Koba-Nielsen-Olesen scaling. The primary cosmic-ray spectrum and composition are extrapolated upwards from the direct measurements made at less than a few TeV. Rates are calculated for detected multiplicities  $n_D = 1-30$  observed over a zenith angle range  $30^\circ-72^\circ$  and over a depth range of  $1.5 \times 10^5-10^6 \text{ g cm}^{-2}$ . Good agreement between predictions and measurements has been obtained with scaling and such a simple extrapolation to higher energies of the directly measured primary spectrum and composition.

### I. INTRODUCTION

One of the outstanding results of the new accelerator experiments has been the success of Feynman scaling<sup>1</sup> and the hypothesis of limiting fragmentation.<sup>2</sup> The failures of scaling are also of great current interest. Using scaling as an analysis framework, very specific predictions can be made for results of collisions in the ultrahigh-energy range studied by cosmic-ray experiments. A successful approach to investigating the predictions of scaling involves the use of data from the Utah Muon Detector.<sup>3</sup> Muons detected far underground are the high-energy remnants of collision processes in the atmosphere and provide information about total inelastic cross sections, multiplicity laws, and the transverse and longitudinal momentum distributions as a function of energy for the various types of secondary particles which produce the observed muons. The muons also provide information about the energy spectrum and composition of the primaries. The challenge, of course, is to be able to unscramble the mixed signals which the muons carry.

A detailed Monte Carlo computer program has been written to aid in the interpretation of the Utah muon data. We use scaling and predict rates of muon events for the various zenith angles, rock depths, and multiplicities seen in the aperture of the Utah detector. It is necessary to make assumptions about the primary cosmic-ray spectrum and composition. We describe here the model which was used and the comparison between predictions and data which provides support for scaling and for an extrapolation (from below  $2 \times 10^3 \text{ GeV}$ ) of the measured spectrum and com-

position into the primary energy region 1 TeV–10 000 TeV. A more complete description of some details of the model and calculation is available.<sup>4</sup>

### II. MODEL

#### A. Nuclear physics

Scaling predicts that for very high collision energies an energy-independent structure function can be found to describe the production of a given type of particle, such as  $\pi^-$  mesons, by protons striking protons. The structure function can be defined as follows:  $f(x, p_T) = E d^2\sigma/dp_L dp_T$ . The quantities  $p_L$  and  $p_T$ , are defined in the nucleon-nucleon center-of-mass (c.m.) frame. The structure function,  $f$ , depends only on the produced particle's transverse momentum,  $p_T$ , and the ratio,  $x$ , of its longitudinal momentum,  $p_L$ , to the maximum value allowed by energy and momentum conservation. The energy of the produced particle is  $E$ ; the relation does not depend on the total collision energy. For high-energy particles produced in the forward hemisphere in the c.m. system,  $x \propto p_L \sim E$  and the following relation exists:  $d^2\sigma/dx dp_T = f(x, p_T)/x$ . For fast particles (in the c.m. frame),  $x$  is to a very good approximation the ratio of the secondary particle's laboratory energy to the incident particle's energy. The inelasticity and  $p_T$  distributions of these particles are independent of the primary energy. In the region for which  $p_L \sim E$ , integration over  $x$  and  $p_T$  gives a logarithmic dependence of the average particle multiplicity on the primary energy if the structure function does not vanish at  $x=0$ .

In order to include effects of the use of a nuclear target (air) in our simulation of atmospheric ha-

dronic cascades, we applied scaling to production cross sections for mesons and nucleons by protons incident on "air nuclei." In view of the scarcity of high-energy inclusive data covering the entire  $x$  and  $p_T$  distributions using nuclear targets, we decided to use a multiparameter fitting function which was successful in describing the entire  $x$  and  $p_T$  kinematic region for  $p$ - $p$  particle production data. This function was then refitted to extensive nuclear target results from an experiment covering a wide range of  $x$  and  $p_T$  values. The nuclear target data used were an interpolation between 19.2-GeV  $p$ -Be and  $p$ -Al data obtained at CERN.<sup>5</sup> Except for a normalization factor of approximately  $A^{2/3}$ , the beryllium and aluminum data are so similar that the interpolation can be expected to give the values for air with about the accuracy of the CERN measurements.

The fits which we made to meson production data used a functional form successfully employed by Bøggild *et al.*<sup>6</sup> to describe 19-GeV  $p$ - $p$  bubble-chamber observations of negative pions. The entire kinematically possible  $x$  and  $p_T$  regions were observable in this experiment without major detection biases. The fitting function we use was therefore a very good representation of the  $x$  and  $p_T$  distribution throughout the kinematic region in which particle production was significant.

The function fitted to the nuclear target data for meson production was

$$E \frac{d^2\sigma}{dp_L dp_T} = f(x, p_T) = \frac{A_1 \exp(-|x|/A_2)}{1 + \exp[(|x| - A_3)/A_4]} \times p_T^{A_5} \exp[-p_T/(A_6 + A_7|x|)] . \quad (1)$$

We evaluated the parameters  $A_1$  to  $A_7$  separately for  $\pi^-$ ,  $\pi^+$ ,  $K^-$ , and  $K^+$  subject to the constraints at  $x=0$  discussed below. Since our only practical

requirement was for Eq. (1) to be a successful fit to the particle production cross sections, we do not offer a particular model which would yield this formula. Some discussion of parameter  $A_5$  is necessary, however. The fits yielded values near 1.5 for this parameter. This is the value given by an approximation to the Hagedorn thermodynamical model.<sup>7</sup> It might be argued that this approximation does not have the proper behavior as  $p_T \rightarrow 0$ , but this consideration is not of great practical significance here because the relative fraction of phase space near  $p_T=0$  is extremely small. It can be seen, for example, in the paper of Bøggild *et al.*,<sup>6</sup> that a fit giving  $A_5$  significantly greater than 1 (1.3 in their case) is a very good approximation to the low- $p_T$  region of the distribution. In our case, the separation of muons from the shower axis is very approximately proportional to  $p_T/p_L$  for the (dominant) pion parents which decay to yield muons. The required distribution  $d^2\sigma/dp_L dp_T$  is adequately fitted with our parameter values. The fits described the data with about 5–10% accuracy for all  $x$  and  $p_T$  values for which the cross sections were not insignificantly small. This is also true for the formula given below which was fitted to the nucleon production data. The results of the fits are summarized in Table I.

A limitation of the nuclear target data we used is that it was all taken at momenta such that  $x \geq 0.35$ . Most of the detected muons are produced by the decay of mesons produced at  $x < 0.35$ . We can compare our predictions at  $x=0$  to CERN Intersecting Storage Rings (ISR)  $p$ - $p$  results. Our average multiplicity of pions in the forward hemisphere of the center-of-mass system is  $1.18 \ln(E/m_p) - 1.3$ . The same quantity measured at ISR is  $1.29 \ln(E/m_p) - 2.5$ .<sup>8</sup> The coefficient of the logarithm is proportional to the integral over  $p_T$  of the structure function at  $x=0$ . Thus we agree within about 9% with the higher-energy  $p$ - $p$  result

TABLE I. Parameter values obtained for particle production cross sections.

	$\pi^-$	$\pi^+$	$K^-$	$K^+$	$p$	
$A_1^a$	15.8 ± 1.8		1.12 ± 0.15	$B_1^a$	4.87 ± 0.50	
$A_5$	1.47 ± 0.04		1.61 ± 0.05	$B_5^b$	-0.149 ± 0.013	
$A_6^b$	0.205 ± 0.008		0.242 ± 0.014			
$A_2$	0.135 ± 0.002	0.176 ± 0.004	0.104 ± 0.002	0.197 ± 0.005	$B_2$	-0.237 ± 0.027
$A_3$	0.677 ± 0.006	0.705 ± 0.006	0.635 ± 0.006	0.763 ± 0.007	$B_3$	1.43 ± 0.04
$A_4$	0.0713 ± 0.0015	0.0710 ± 0.0016	0.045 ± 0.003	0.064 ± 0.003	$B_4^b$	0.285 ± 0.012
$A_7^b$	-0.045 ± 0.009	-0.048 ± 0.009	-0.133 ± 0.021	-0.072 ± 0.016		

<sup>a</sup> In units of barns  $\text{GeV}^{-1} c^2$ .

<sup>b</sup> In units of  $\text{GeV} c^{-1}$ .

for pion production at  $x=0$ . However, unknown nuclear target effects near  $x=0$  may still not be accurately represented by our fitting procedure.

The production of protons in the final state was described by a somewhat different five-parameter fit:

$$\frac{d^2\sigma}{dx dp_T} = B_1(1 - |x|)^{B_2} p_T^{B_3} \exp[-p_T/(B_4 + B_5|x|)]. \quad (2)$$

The proton fit assumed that the proton  $x$  and  $p_T$  distributions were energy-independent for all  $x$  values. As described below, production of nucleon-antinucleon pairs was treated as a separate process.

As indicated in Table I, the structure functions of mesons of opposite charge were constrained to be equal at  $x=0$ . This was done in order to avoid logarithmically divergent violations of charge and strangeness conservation at asymptotic energies. For all energies the fits satisfy energy, strangeness, charge, and baryon conservation satisfactorily. Neutrons were assumed to have the same  $x$  and  $p_T$  dependence as protons, but to be produced only 77% as frequently as protons in  $p$ -air collisions. Hyperons were assumed to be included implicitly in the distributions through their decay products. The additional contribution of nucleon-antinucleon pairs was included in an approximate fashion based on the similarity in the shapes of the  $x$  distributions for antiprotons and  $K^-$  as observed at the ISR for  $p$ - $p$  collisions.<sup>9</sup>

In practice (although not in the fits summarized in Table I) we modified the pion distributions in the region  $x < 0.35$  to agree with the  $x$  dependence of the average transverse momentum observed at 12 and 24 GeV in proton-proton interactions (the so-called "seagull effect").<sup>9</sup> The essential feature of the "seagull effect" is that, when averaged over invariant phase space, the average transverse momentum falls steadily as one approaches  $x=0$  from  $x=0.35$ . We scaled our  $p_T$  distributions for mesons to give this dependence. This has the consequence of lowering the over-all multiplicity of produced pions and of lowering the mean transverse momentum averaged over all  $x$  from the values following from direct use of the parameter values in Table I.

We thus obtain an average  $p_T$  value for all pions with  $x \geq 0.01$  of 0.38 GeV/ $c$ . The calculated mean inelasticity of the incident nucleon is 0.58, which is somewhat higher than for  $p$ - $p$  collisions. The average number of pions of all three charge states and for the forward hemisphere only is  $\langle n_\pi \rangle = 1.18 \times \ln(E/m_p) - 1.3$ . The average number of kaon pairs used (all charge states, forward hemisphere) is

$\langle n_K \rangle = 0.114 \ln(E/m_p) - 0.39$ . For the number of antiprotons (both hemispheres) we used  $\langle n_{\bar{p}} \rangle = -0.37 + 0.059 \ln s + 0.75/s^{1/2}$ , where  $s$  is the square of the c.m. energy.<sup>8</sup>

The particle multiplicity distribution given by Slattery<sup>10</sup> is used in the calculation. This distribution follows the Koba, Nielsen, and Olesen<sup>11</sup> (KNO) scaling hypothesis for multiplicity distributions. Assuming Feynman scaling, Koba *et al.* argued that the relative fraction of final-state events with  $n$  charged particles,  $\sigma_n/\sigma_{\text{inel}}$ , should asymptotically obey

$$\frac{\sigma_n}{\sigma_{\text{inel}}} \xrightarrow{s \rightarrow \infty} \langle n \rangle^{-1} \chi(n/\langle n \rangle). \quad (3)$$

Thus an energy-independent function,  $\chi$ , could be found which would give the charged-particle multiplicity distribution at all (very high) collision energies by use of this scaling law. Slattery found that this scaling law is already valid at relatively low energies, for beam momenta of 50–300 GeV/ $c$  in  $p$ - $p$  collisions. We used the  $\chi$  function as fitted to data by Slattery for the distribution of numbers of charged particles. We also assumed that the number of neutral particles, which rarely produce muons, is always equal to the average number. To facilitate the preservation of energy independence of the particle  $x$  distribution for  $x > 0.01$ , a Poisson distribution of particle multiplicities is used in this region. The number of particles with  $x < 0.01$  is then given by the difference of a number given by the Slattery distribution and the number of particles with  $x > 0.01$ . The results of the calculations are observed to be relatively insensitive to the details of this procedure.

In the development of hadronic cascades in the atmosphere, mesons frequently become the incident particles in secondary collisions. A quark model has suggested that forward-hemisphere particle distributions in meson-proton collisions are related to those in  $p$ - $p$  collisions.<sup>12</sup> For forward-hemisphere particles, the  $x$  values of produced particles (excluding leading particles) in proton collisions are multiplied by  $\frac{3}{2}$  to give the  $x$  values for meson-proton collisions. Comparison of bubble-chamber data for incident protons and mesons supports this prescription. It has been extended to relate meson-air collisions to  $p$ -air collisions. Its validity does not depend on the validity of the quark model which suggests it, and the scaling assumption ensures its validity at all energies. In roughly one-half of the meson-induced collisions a leading meson is provided from a protonlike momentum distribution. Compared to  $p$ -air collisions, this lower frequency of leading particles in meson-air collisions, together with

higher  $x$  values of produced particles, allows energy to be conserved in the meson-air collisions.

A method has been developed to generate interactions by the Monte Carlo process which preserves the desired multiplicity and inclusive  $x$  distributions and which conserves energy for each interaction. Correlations of the particles in an interaction are introduced only incidentally in the process of conserving the energy in the interactions. However, the Monte Carlo results to be discussed in Sec. V show that in most events with two muons in the detector the muons come from hadrons produced in separate collisions. Consequently, the effect on multiple-muon event rates of two-particle correlations in the actual  $p$ -air collisions is expected to be small.

We have assumed that inelastic cross sections are rising with energy with the dependence suggested by Gaisser and Yodh.<sup>13</sup> The inelastic cross sections for particles other than protons colliding with air are assumed to rise in a similar manner. We used the following values:

$$\sigma_{p\text{-air}} = 280 \text{ mb} + 2.5 \ln^{1.8}(E/100 \text{ GeV}), \quad (4)$$

$$\sigma_{\pi\text{-air}} = 196 \text{ mb} + 1.7 \ln^{1.8}(E/67 \text{ GeV}), \quad (5)$$

$$\sigma_{\alpha\text{-air}} = 442 \text{ mb} + 3.9 \ln^{1.8}(E/100 \text{ GeV}), \quad (6)$$

$$\sigma_{K\text{-air}} = 178 \text{ mb} + 1.6 \ln^{1.8}(E/67 \text{ GeV}). \quad (7)$$

#### B. Spectrum, composition, and nuclear fragmentation

We assume that the spectral shapes of the components of the primary flux (protons,  $\alpha$ 's, and a mixture of heavier nuclei) follow power laws of the form  $AE^{-\gamma}$ . ( $A$  will be referred to as the "amplitude" and  $\gamma$  as the spectral index.) The amplitude and spectral index are allowed to vary in the work that follows. The amounts of heavier nuclei are taken to be constant relative to protons. The ratios are taken from a synthesis of measurements at energies ranging from 2 GeV per nucleon to 500 GeV per nucleon. ( $Z=2$ , Ryan *et al.*<sup>14</sup>;  $Z=2-9$ , Cartwright *et al.*<sup>15</sup>;  $Z=10-28$ , Shapiro and Silberberg<sup>16</sup>;  $Z=26$ , Balasubrahmanyam and Ormes.<sup>17</sup>) This gives 0.042 for the ratio of helium to protons at the same energy per nucleon. The iron group intensity relative to protons was taken to be the value measured near 100 GeV per nucleon, the highest energy reported by the Goddard group.

When an alpha particle is the primary cosmic ray, it is assumed that it will fragment into individual nucleons in the first interaction. The number of projectile nucleons which participate in the interaction is selected according to a calculated distribution from Faeldt *et al.*<sup>18</sup> The probabilities for 1 through 4 nucleons interacting are 0.33, 0.49,

0.04, and 0.14, respectively. The heavier primaries are allowed to break up in a series of collisions in the atmosphere based upon fragmentation probabilities from Shapiro and Silberberg.<sup>16</sup> Half of the free nucleons (i.e., not bound in fragment nuclei) produced in each collision are assumed to interact in that collision, this being a simple generalization of the theoretical result<sup>18</sup> for the number of participating nucleons in alpha-particle-nitrogen collisions.

Much of the effect of using our particular nuclear breakup model can be summarized by giving the effective mean free paths we obtain for nucleons bound in nuclei entering the earth's atmosphere. These are the average depths nucleons reach before interacting. The individual nucleon-air interaction, when it occurs, is assumed to have the same characteristics as an inelastic  $p$ -air interaction. At energies near  $10^{12}$ - $10^{14}$  eV/nucleon, the effective mean free path is 86 g/cm<sup>2</sup> for incident helium nuclei. For nuclei with  $3 \leq Z \leq 14$  (mainly C, N, and O), the value is about 88 g/cm<sup>2</sup>, and for nuclei with  $15 \leq Z \leq 26$  (mainly Cr and Fe) it is about 92 g/cm<sup>2</sup> at energies near  $10^{12}$ - $10^{14}$  eV/nucleon. For comparison, the proton mean free path is 76 g/cm<sup>2</sup> from Eq. (4) in this energy region. The effective mean free paths are all quite similar, and our results would be expected to be close to those obtained by simply adding the effects of  $A$  independent nucleon showers to approximate the shower produced by a nucleus of atomic weight  $A$  at a given energy per nucleon.

#### C. Particle propagation

Inasmuch as the altitude of interaction influences the spatial extent of a shower of muons observed underground in the Utah experiment (thus influencing the directly observed multiplicity distribution and separation of muons), some effort must be made to account for the details of atmospheric structure. In this work we have adopted the density distribution of the standard atmosphere by Berry *et al.*<sup>19</sup> We take the Wasatch Mountains to be (on the average, near the detector) at an atmospheric depth of 750 g cm<sup>-2</sup> corresponding to an altitude of 2.62 km. By far, the majority of muons arise from collisions in the stratosphere, which extends to a vertical depth of 240 g cm<sup>-2</sup> (corresponding to an altitude of 10.8 km). If  $h$  is the slant depth (in g cm<sup>-2</sup>) into the atmosphere at zenith angle  $\theta$ , then the density of the atmosphere is given by

$$\frac{(h \cos \theta) \times 10^{-5}}{6.335} \text{ g cm}^{-3} \quad (8)$$

stratosphere, altitude > 10.8 km,

$$\frac{(h \cos \theta)^{0.81}}{225445} \text{ g cm}^{-3} \quad (9)$$

troposphere, altitude  $\leq 10.8$  km .

For zenith angles beyond  $70^\circ$  (our  $72.5^\circ$  data are only slightly affected by this) the factor  $(h \cos \theta)$  must be replaced by a factor which compensates for the curvature of the atmosphere about a spherical earth. Tables for this purpose are taken from Osborne,<sup>20</sup> and our method yields values good to an estimated 5% for vertical depths exceeding  $2 \text{ g cm}^{-2}$  and zenith angles less than  $84$  degrees.

Knowledge of the density of the atmosphere is necessary for the computation of interaction and decay probabilities. The question which must be answered for each meson at a depth  $h$  in the atmosphere is: Where will the next interaction or decay occur? Approximations necessary to answer this question in a minimum of computation time lead to errors which are greatest in the region where  $h$  is small. When the original position of the meson, for example, is  $2 \text{ g cm}^{-2}$ , the error in the final depth is roughly 10%. In the troposphere, where only a few of the muons relevant to our calculation are produced, errors in the final depth for a meson starting at position  $h$  are of the order of 5%. In the depth region where most mesons are produced, the errors are less than 5%.

In order to calculate event rates we need probabilities that muons of a given surface energy will reach the rock depth of the detector. We use underground muon survival probabilities calculated by Carlson.<sup>21</sup> The muon energy losses he used are described by Carlson and Morrison<sup>22</sup> along with an improved value of bremsstrahlung energy loss. These are based on calculations of bremsstrahlung and pair-production cross sections in nuclear collisions and of photonuclear interactions by Petrukhin and Shestakov,<sup>23</sup> Kokoulin and Petrukhin,<sup>24</sup> and Cassidy,<sup>25</sup> respectively. The average muon energy-loss rates we used for standard rock are shown in Fig. 1 for processes other than ionization. In calculating survival probabilities, Carlson used a bremsstrahlung average energy-loss rate of  $-E^{-1}dE/dh \approx 1.7 \times 10^{-6} \text{ g}^{-1} \text{ cm}^2$  at all energies instead of improved values which are lower at lower energies. To correct for this difference we multiplied our calculated event rates at each depth by a correction factor. These calculated factors increase with depth from 1.06 to 1.20 over the range of depths we consider.

Multiple scattering effects were estimated for the entire muon trajectory and geomagnetic effects were included for hadron and muon trajectories in the atmosphere. These are small, but not insignificant, corrections for some aspects of the calculation.

### III. CALCULATIONS

The model has been used to predict rates of events observed in the Utah muon detector. The three variables on which the rates depend are the angle,  $\theta$ , between the shower axis and the zenith, the total depth,  $h$ , in the direction of the shower axis, and the number of muons,  $n_D$ , detected in the event. The rates have been predicted for four angular regions and at those depths (in steps of  $8 \times 10^4 \text{ g cm}^{-2}$ ) at which measurements are possible at the various angles. The rates of measured events have been determined for the angles  $30^\circ$ ,  $47.5^\circ$ ,  $62.5^\circ$ , and  $72.5^\circ$  by Lowe *et al.*<sup>3</sup> The angles at which the predictions were made were chosen to span as broad a range of data as possible with a limited number of predictions. The rates were calculated for all  $n_D$  values for which the Monte Carlo predictions were not unreasonably expensive.

In the Monte Carlo calculation the primary spectrum was divided into segments of 1–2 TeV per nucleon, 2–4 TeV per nucleon, 4–8 TeV per nucleon, etc. Primary protons of, for example, 512–1024 TeV are in segment 10. Calculations for the contribution of each energy segment to rates of muons of all multiplicities were done independently, and moreover, the calculations were done independently for pure primary protons, pure alpha particles, and heavier nuclei. Within each energy segment the primary spectrum was assumed to fall as  $dN/dE_0 \propto E_0^{-2.7}$ . The independence of the predictions for different energy segments and chemical components allows the approximate effects of various possible spectrum and composition assumptions to be evaluated without

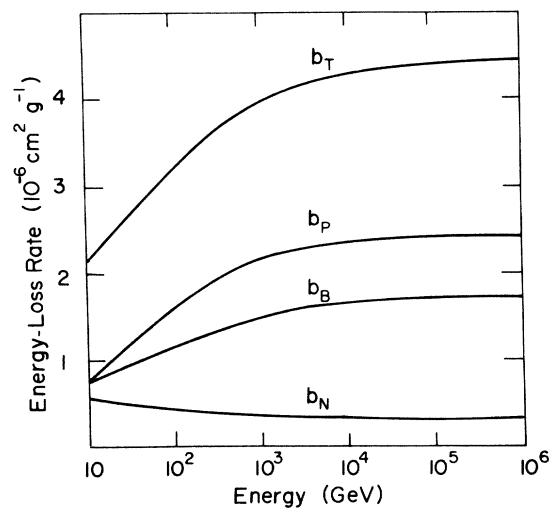


FIG. 1. Muon average energy loss rates  $b = -E^{-1}dE/dh$  for standard rock for nuclear, bremsstrahlung, and pair-production losses and their sum  $b_T$ .

repeating the basic Monte Carlo calculations. This is done by adding all appropriately weighted predictions of the different components and energy segments to obtain a prediction for an altered primary spectrum or primary composition. Experience in the operation of the Monte Carlo program has shown which segments contribute significantly to a rate prediction and comparisons to measurements are only made for those rates for which all significant contributions have been calculated.

The predictions for the rates are made in several stages. In the first stage the air showers are generated at a given zenith angle and muons are produced in the atmosphere. Muons and hadrons are dropped from the shower if they have energies below the lowest muon threshold energy of interest.

In a second stage, the showers produced in the first stage are analyzed at the various depths present at the zenith angle being considered. The analysis determines the yield (per shower) of events with given  $n_D$ ,  $\theta$ , and  $h$  values produced by a given primary energy segment and primary constituent. For  $n_D < 10$ , Lowe et al.<sup>3</sup> have corrected their data to give event rates for an 80-m<sup>2</sup> detector area perpendicular to the incident shower direction. For these low-multiplicity muon events the rate analysis integrates over all possible shower-axis locations relative to the center of a rectangular 8×10-m<sup>2</sup> detector fiducial area. For  $n_D > 10$ , the experimental data were given for a 100-m<sup>2</sup> detector area perpendicular to the shower direction. For these high-multiplicity events the rate analysis uses a method of sampling a limited number of shower-axis locations relative to the center of the 10×10-m<sup>2</sup> detector fiducial area used in the high-multiplicity experimental analysis. The two analysis techniques have been checked against each other and are consistent with each other.

In the third and last stage of the calculation, the rates of events are predicted. A contribution to a rate for a given  $n_D$ ,  $\theta$ , and  $h$  is found by multiplying the yield per shower of that type of event by the rate of showers from the energy segment and primary constituent being considered.

#### IV. EVENT-RATE PREDICTIONS

##### A. Comparison to measurements

Our predictions were fitted to the measured event rates with two primary spectrum parameters left free. These are the amplitude  $A$  of the proton component and the spectral index  $\gamma_1$ . The rigidity  $R$  of a break in the slope of each component of the primary spectrum above which the spectral index,  $\gamma_2$ , is set equal to 3.3 was fixed at  $3 \times 10^{15}$  V. The results of exploratory fits were found to be very

insensitive to the location of the break. The best-fit values  $A = (2.3 \pm 0.2) \times 10^4 \text{ GeV}^{-1} \text{ m}^{-2} \text{ sec}^{-1} \text{ sr}^{-1}$  and  $\gamma_1 = 2.75 \pm 0.02$  are in reasonable agreement with the balloon-flight measurements of Ryan et al.<sup>14</sup> who found  $A = (2.0 \pm 0.2) \times 10^4 \text{ GeV}^{-1} \text{ m}^{-2} \text{ sec}^{-1} \text{ sr}^{-1}$  and  $\gamma = 2.75 \pm 0.03$  for proton energies up to about  $10^{12}$  eV. This indicates the reasonableness of extrapolating the primary spectrum from lower energies to the higher energies studied in this experiment. The  $\chi^2$  for the fit was 36.5 for 30 degrees of freedom.

The results of the two-parameter fit of our predictions to the measurements are shown in Fig. 2, and the values of the predictions and measurements are given in Table II. In Fig. 2 the error bars are the combination of the Monte Carlo statistical uncertainties and the measurement uncertainties. The measurement uncertainty calculation is described in Ref. 3. The curves drawn through the Monte Carlo predictions show events as a function of  $n_D$  for the four angular regions in which the comparisons were made. The depths at which data are available in an angular region are determined by the detector orientation and the shape of the mountainous terrain above the detector. In addition, of course, the depths must not be too great or the rates are too low to be measurable. In the case of  $n_D = 1$ ,  $\theta = 72.5^\circ$ ,  $h = 8.0 \times 10^5 \text{ g cm}^{-2}$  events only, the measurements are taken in an angular region ( $75^\circ - 85^\circ$ ) away from the quoted values and are extrapolated to  $72.5^\circ$  using calculated angular-dependence factors.<sup>21</sup> The estimated error due to this procedure is small compared to the experimental uncertainty of this measurement.

The ratios of the predicted to the measured rates are shown in Fig. 3. This illustrates the agreement and disagreement of the predictions and measurements more clearly than Fig. 2. In most cases the agreement is good. The predicted single-muon rate, however, is high at greater angles and depths. A similar behavior was noted in an earlier separate analysis<sup>21</sup> of the depth and angular dependence of the underground muon intensity (which is similar to the singles rate of our detector) by Carlson, who found that a steepening of the primary spectrum with increasing energy per nucleon was necessary to obtain a satisfactory fit extending to deep depths. It should be noted, however, that the sensitivity to uncertainties in muon energy-loss rates and in rock density is greatest for the deep single-muon measurements.

A rough estimate of sensitivity to uncertainties in the energy-loss rate of muons per unit depth can be made by neglecting the change in muon range fluctuations and only considering the more significant uncertainties in the range of muons with a given energy and an average energy loss. These

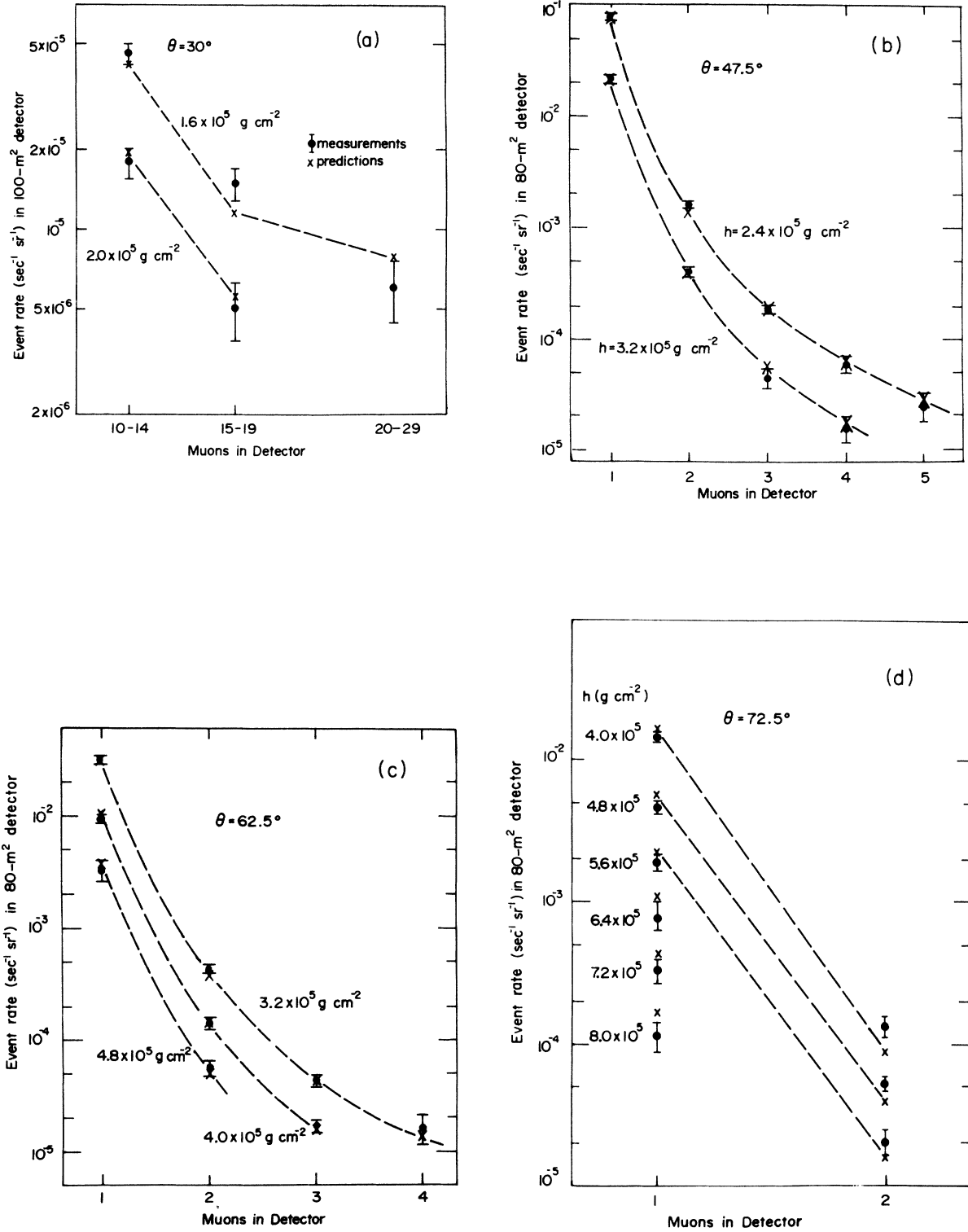


FIG. 2. Comparison of fit of scaling predictions to muon event rates at four zenith angles. The error bars on the measurement points show the combined measurement errors and statistical errors of the Monte Carlo predictions. The predictions, measurement values, and error estimates are listed in Table II.

TABLE II. Comparison of fitted predictions to measurements in an 80-m<sup>2</sup> detector for  $n_D < 10$  and in a 100-m<sup>2</sup> detector for  $n_D \geq 10$ .

Zenith angle (deg)	Depth (10 <sup>5</sup> g cm <sup>-2</sup> )	$n_D$	Measured rate <sup>a</sup> (sec <sup>-1</sup> sr <sup>-1</sup> )	Predicted rate <sup>b</sup> (sec <sup>-1</sup> sr <sup>-1</sup> )
47.5	2.4	1	$(0.786 \pm 0.040) \times 10^{-1}$	$(0.746 \pm 0.027) \times 10^{-1}$
		2	$(0.158 \pm 0.010) \times 10^{-2}$	$(0.136 \pm 0.006) \times 10^{-2}$
		3	$(0.182 \pm 0.014) \times 10^{-3}$	$(0.197 \pm 0.008) \times 10^{-3}$
		4	$(0.592 \pm 0.094) \times 10^{-4}$	$(0.614 \pm 0.027) \times 10^{-4}$
		5	$(0.251 \pm 0.070) \times 10^{-4}$	$(0.273 \pm 0.013) \times 10^{-4}$
	3.2	1	$(0.214 \pm 0.015) \times 10^{-1}$	$(0.211 \pm 0.009) \times 10^{-1}$
		2	$(0.398 \pm 0.034) \times 10^{-3}$	$(0.395 \pm 0.021) \times 10^{-3}$
		3	$(0.439 \pm 0.077) \times 10^{-4}$	$(0.526 \pm 0.024) \times 10^{-4}$
		4	$(0.159 \pm 0.041) \times 10^{-4}$	$(0.174 \pm 0.010) \times 10^{-4}$
62.5	3.2	1	$(0.313 \pm 0.022) \times 10^{-1}$	$(0.295 \pm 0.009) \times 10^{-1}$
		2	$(0.425 \pm 0.033) \times 10^{-3}$	$(0.367 \pm 0.026) \times 10^{-3}$
		3	$(0.424 \pm 0.048) \times 10^{-4}$	$(0.463 \pm 0.025) \times 10^{-4}$
		4	$(0.162 \pm 0.048) \times 10^{-4}$	$(0.138 \pm 0.007) \times 10^{-4}$
	4.0	1	$(0.912 \pm 0.080) \times 10^{-2}$	$(1.01 \pm 0.05) \times 10^{-2}$
		2	$(0.138 \pm 0.012) \times 10^{-3}$	$(0.137 \pm 0.013) \times 10^{-3}$
		3	$(0.170 \pm 0.018) \times 10^{-4}$	$(0.152 \pm 0.009) \times 10^{-4}$
	4.8	1	$(0.331 \pm 0.070) \times 10^{-2}$	$(0.363 \pm 0.020) \times 10^{-2}$
		2	$(0.552 \pm 0.080) \times 10^{-4}$	$(0.513 \pm 0.041) \times 10^{-4}$
	72.5	4.0	1	$(0.146 \pm 0.011) \times 10^{-1}$
2			$(1.34 \pm 0.24) \times 10^{-4}$	$(0.881 \pm 0.044) \times 10^{-4}$
4.8		1	$(0.465 \pm 0.044) \times 10^{-2}$	$(0.540 \pm 0.026) \times 10^{-2}$
		2	$(0.518 \pm 0.059) \times 10^{-4}$	$(0.390 \pm 0.027) \times 10^{-4}$
5.6		1	$(0.190 \pm 0.022) \times 10^{-2}$	$(0.218 \pm 0.013) \times 10^{-2}$
		2	$(0.202 \pm 0.038) \times 10^{-4}$	$(0.161 \pm 0.016) \times 10^{-4}$
6.4		1	$(0.773 \pm 0.118) \times 10^{-3}$	$(0.957 \pm 0.086) \times 10^{-3}$
7.2		1	$(0.328 \pm 0.046) \times 10^{-3}$	$(0.396 \pm 0.044) \times 10^{-3}$
8.0		1	$(0.113 \pm 0.018) \times 10^{-3}$	$(0.169 \pm 0.020) \times 10^{-3}$
30.0		1.6	10-14	$(0.456 \pm 0.036) \times 10^{-4}$
	15-19		$(0.147 \pm 0.019) \times 10^{-4}$	$(0.116 \pm 0.008) \times 10^{-4}$
	20-29		$(0.600 \pm 0.130) \times 10^{-5}$	$(0.787 \pm 0.088) \times 10^{-5}$
	2.0	10-14	$(0.177 \pm 0.020) \times 10^{-4}$	$(0.192 \pm 0.013) \times 10^{-4}$
		15-19	$(0.500 \pm 0.110) \times 10^{-5}$	$(0.562 \pm 0.055) \times 10^{-5}$

<sup>a</sup> The measured rates and estimated errors are obtained from G. H. Lowe, M. O. Larson, H. E. Bergeson, J. W. Cardon, J. W. Keuffel, and J. West, preceding paper, Phys. Rev. D **12**, 651 (1975).

<sup>b</sup> The error estimates for the predictions include only the statistical fluctuations in the Monte Carlo calculation.



uncertainties have a magnified effect on muon rates because of the steeply falling muon spectrum. To first order the magnification factor for fractional errors in a given rate  $J(n_D)$  is  $d \ln J / d \ln h$ . It increases from about 4 to 9 as the depth increases from  $2.4 \times 10^5$  to  $8 \times 10^5$   $\text{g cm}^{-2}$ .

In order to test for the effects of uncertainties in muon range, we have used the muon range estimates of Wright.<sup>26</sup> These were obtained by assuming an uncertainty in the muon energy-loss rate of 1% for ionization losses, which dominate at low energies, and of nearly 10% for the remaining losses, which dominate at high energies. Combining such an energy-dependent increase or decrease in range with the depth dependence of muon rates changes the best-fit values of  $A$  by  $-13\%$  and  $+29\%$  and gives new best-fit values of 2.78 and 2.75 for  $\gamma$ . Because of the wide range of primary energy corresponding to different muon multiplicities at shallow depths, the change in  $\gamma$  is remarkably small. The goodness of fit varies significantly, as does the predicted depth dependence of the singles, which were measured over the widest range of depths. Increasing our muon energy losses by about half of Wright's uncertainty produced a best fit with  $A$  increased by 13% and with a  $\chi^2$  of 29 for the 29 degrees of freedom. The small change for  $\gamma$  observed here is in marked contrast to the uncertainty in spectral shape which arises when only the underground muon intensity is studied and energy-loss uncertainties are considered.<sup>21</sup>

The rock density might also be somewhat higher than expected in the rather restricted directions in which the greatest depths occur, causing the measured single-muon rate to be somewhat lower than expected. Some support for this possibility is given by a comparison of the Kolar-Gold-Field (KGF) measurements of deep underground muon intensities<sup>27</sup> to the Utah measurements. The somewhat larger KGF intensities beyond  $7 \times 10^5$   $\text{g cm}^{-2}$  are in better agreement with our single-muon rate predictions. Other possible causes of the systematic discrepancies between the measurements and predictions are discussed in the next section.

#### B. Sensitivity to the interaction model

In light of the sensitivity of our predictions to what are at present poorly known input parameters, the discrepancies between some of the predictions and measurements are not regarded as serious. The  $\chi^2$  value given above was obtained with the measurement errors combined with the statistical errors of the Monte Carlo predictions. The systematic errors arising from the uncertainties of

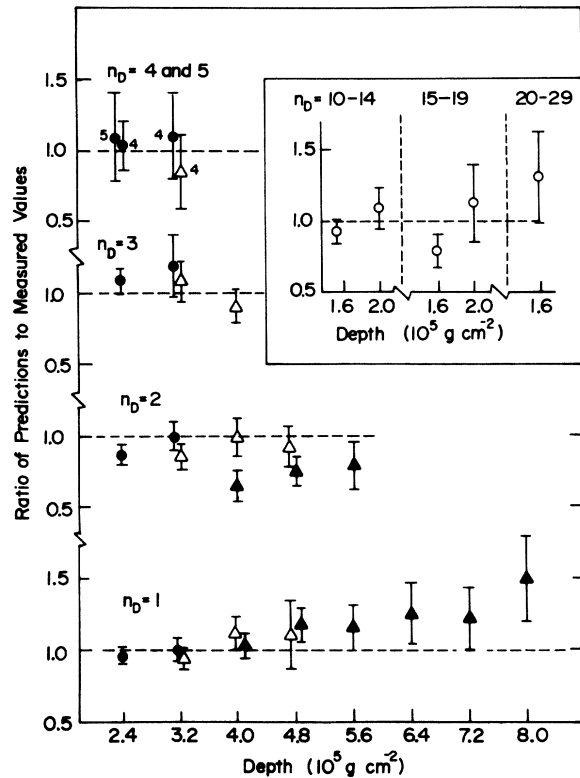


FIG. 3. Depth dependence of ratios of predicted to observed muon event rates. Data at zenith angles of  $30^\circ$ ,  $47.5^\circ$ ,  $62.5^\circ$ , and  $72.5^\circ$  are represented by open circles, solid circles, open triangles, and solid triangles, respectively.

the predictions were not included. These neglected errors come from uncertainties in the inputs of the Monte Carlo program. They include the neglected energy dependence of the structure functions above 19 GeV (where scaling is only approximately valid) and the lack of completeness of required sets of measurements. In particular, measurements are scarce for the inclusive neutron cross section. The  $x$  and  $p_T$  dependences of the neutron inclusive cross section were approximated by the distribution fitted to the proton inclusive distribution.

An estimate of the effect of using a neutron  $x$  dependence given by Bassetto and Dias de Deus<sup>28</sup> indicates that the predictions are sensitive to the assumed secondary-neutron inclusive cross sections. The factors by which this modification changed the predicted rates of muon events were calculated at three depth angle combinations for proton primaries. Using these same factors for heavier primaries, we obtained improved agreement with the measurements for events at  $72.5^\circ$  with  $n_D = 2$  and small effects for the other predic-

tions.

Because the ISR neutron results of Engler *et al.*<sup>29</sup> are quite different from the 24-GeV *p*-Be neutron results<sup>30</sup> reported earlier by the same group, and because the total inclusive neutron cross section from the ISR measurements appeared lower<sup>28</sup> than expected from baryon conservation together with the ISR inclusive proton multiplicities given by Antinucci *et al.*,<sup>8</sup> it was decided that modifications of our approximation for inclusive neutron production would not be attempted at present.

Several other tests of the sensitivity of the predictions to modifications of the model have been done. One test involved replacing the energy-dependent total cross section by a constant value of 335 mb for the calculation. This is the highest value given by the analysis of Yodh, Pal, and Trefil<sup>31</sup> and was obtained by them at the highest energy at which they analyzed data, near 10 TeV. For  $n_D = 1-5$  at  $\theta = 47.5^\circ$  and  $h = 2.4 \times 10^5 \text{ g cm}^{-2}$ , the changes of the predictions were not large enough to be significant in comparison to the combined statistical fluctuations of the two Monte Carlo calculations.

Another sensitivity test involved the increase of the  $p_T$  values of all shower particles by 25% to test the effect on the rate predictions of scaling up all  $p_T$  values in this energy range. For  $n_D = 2-5$ ,  $\theta = 47.5^\circ$  and  $h = 2.4 \times 10^5 \text{ g cm}^{-2}$ , the modified predictions were found to be increasingly lower than the unmodified set as  $n_D$  increased, until a 36% decrease was observed at  $n_D = 5$ . For  $n_D = 1$  no change was observed. These changes are in qualitative agreement with the effect which might be expected due to the greater separation of muons in showers when  $p_T$  is increased. This particular result indicates a moderate sensitivity to change of the  $p_T$  distribution at higher energies. It should be emphasized, however, that if the  $p_T$  distribution is unchanged up to  $\approx 1 \text{ GeV}/c$  but occasionally particles of very high  $p_T$  occur, the rates of multiple-muon events are not expected to be significantly affected. Our analysis shows, however, that the measured multiple-muon rates do not require greatly increased  $p_T$  values in this energy range.

## V. OTHER RESULTS OF THE CALCULATION

### A. Primary cosmic-ray energies producing observed events

The median energy of primary cosmic rays which produced underground muon events are found in our calculations. The energies depend weakly on the assumed primary spectrum, and the results given below are obtained from the spectral

slope determined by our best fit to the primary spectrum.

Figure 4 shows the dependence on  $n_D$  and  $h$  of the median parent energies of muon events produced by primary protons. Results are, at most, weakly dependent on the zenith angle,  $\theta$ , and this dependence of the parent energies was ignored. For any fixed  $n_D$ , the median parent energies are seen to increase as rock depth at detection increases. A wider variation of primary energies is found by studying events of different  $n_D$  values. At fixed  $h$ , the median parent energies increase rapidly as the  $n_D$  value is increased. The median energies of events produced by parent protons extend up to about  $6 \times 10^{15} \text{ eV}$  for the highest  $n_D$  values for which comparisons of predictions and measurements have been made. It is also important to note that there is significant overlapping of different  $n_D$  values at a given value of the parent energy. This implies that an interaction model may not be able to obtain agreement with the measurements simply by variation of the assumed primary spectral slope because the model must successfully predict the ratios of rates for different  $n_D$  values at the same primary energy. For example, the model must successfully predict the relative rates with  $n_D = 3, 4, 5,$  and  $10-14$  near  $1-2 \times 10^{15} \text{ eV}$ .

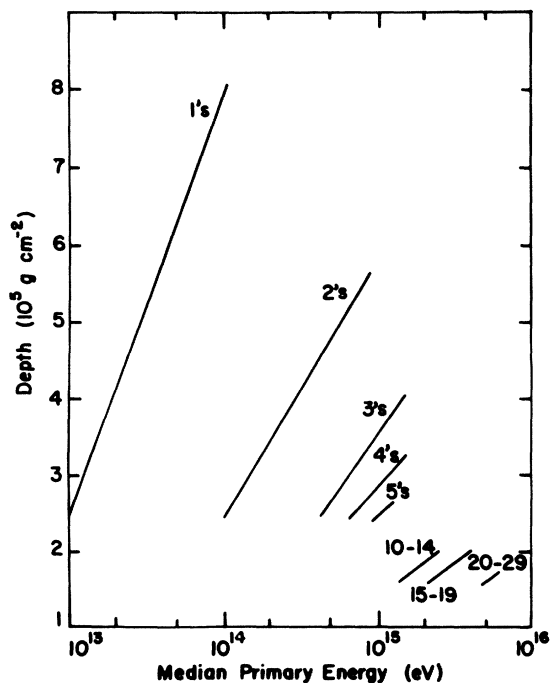


FIG. 4. Calculated depth dependence of median energy of primary protons which produce events with the indicated multiplicities of observed muons.

The primary composition which we have assumed for our comparison to the measurements includes heavy nuclei in addition to protons. Figure 5 shows the median values of the energy per nucleon for primary nuclei with  $Z > 2$  which produce underground muon events. At each depth, the median energy per nucleon for primary heavy nuclei producing *single*-muon events is close to the median energy of protons producing such events. This is the expected result if muon production by a nucleus of atomic weight  $A$  can be treated as approximately equal to the muon production from a superposition of  $A$  proton showers.

In the case of underground muon events with 2 or more muons the median energy per nucleon of the primary is lower for production by heavy nuclei than for production by protons. In some examples the total median energy of the primary particle (the entire nucleus) is similar for incident iron and proton primaries, but this is not accurately true in all cases. For the study of nuclear interaction models, the energy per nucleon may be the most important variable, and it is for this reason that the energy per nucleon rather than the total particle energy was given in Fig. 5. Certainly, for  $n_D \geq 2$ , a large fraction of the produced muons result from collisions of nucleons freed from nuclei in previous collisions. These nucleons carry energy equal to or less than the energy per nucleon of the primary cosmic ray.

#### B. Contributions of different generations of the hadronic cascade

In the case of  $n_D = 1$ , the rapidly falling primary spectrum favors production of muons in the most efficient way possible, i.e., by decay of mesons produced at higher-than-average  $x$  values in the first collision of the primary cosmic-ray particles with nitrogen or oxygen nuclei in the atmosphere. In fact, most single-muon events come from these "first-generation" particles.

When events with  $n_D \geq 2$  are considered, however, the most important production process is not decay of several first-generation mesons. Second- and higher-generation mesons, produced by the second- or higher-generation collisions of nucleons and mesons are very important sources of muons for  $n_D \geq 2$ . For  $n_D = 2$ , most muons come from generations 1 to 3. For multiplicity  $n_D = 4$ , with proton primaries, most muons come from generations 2 to 5. For  $n_D \geq 2$  events from primary heavy nuclei, the mean number of generations involved is less than for production by protons. Because of the importance of a number of generations in the hadronic cascade, the multiple-muon events from a given median primary energy

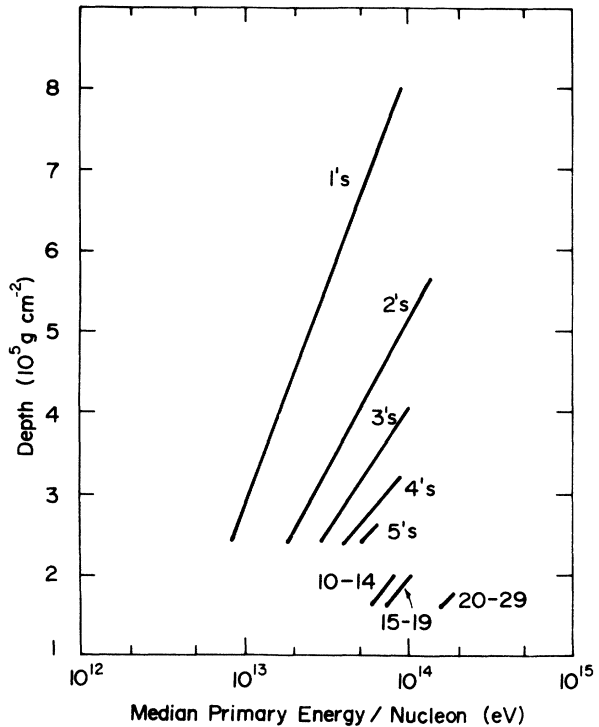


FIG. 5. Calculated depth and multiplicity dependence of the median primary energy/nucleon for events produced by primary nuclei with  $Z > 2$ .

are sensitive to interaction characteristics in a wide range of energies.

#### C. Contributions of different primary components

Figure 6 shows the contributions of different primary components to the rates of our events with  $n_D = 1$  to 5 for  $\theta = 47.5^\circ$  and  $h = 2.4 \times 10^5 \text{ g cm}^{-2}$ . The trends at other angles and depths are quite similar. The contribution of a component is proportional to the product of the probability of occurrence of this component and the effectiveness of the component for production of the given type of event. It is clear that single-muon events are produced primarily by primary protons. From the previous discussion, the relative importance of the primary protons for single-muon production should be approximately equal to the fraction of primary nucleons of a given energy which occur as free protons. For our assumed composition this fraction is 78%, which is close to the 80% obtained for the actual calculated contribution to single-muon production.

Figure 6 shows that the relative contribution from heavier nuclei increases as  $n_D$  increases. But even for  $n_D = 5$  the contribution of the protons is not negligible. When events having different  $n_D$

values (at different rock depths) result from similar primary energies, the relative event rates depend on the primary composition. The multiple-muon rates therefore constrain the primary composition as well as the primary spectrum, if a specific interaction model can be assumed. In the present analysis the consistency of the measurements and the predictions was checked in the context of an energy-independent primary composition.

## VI. CONCLUSIONS AND DISCUSSIONS

Predictions of underground muon event rates based on Feynman scaling and KNO multiplicity scaling have been found to be quite successful in obtaining agreement with measurements made on cosmic-ray showers of energies from about  $2 \times 10^{12}$  eV up to above  $10^{15}$  (see Ref. 32). The primary composition was assumed to be the same as measured at energies several orders of magnitude lower and the primary cosmic-ray energy spectrum was fitted to the measurements giving parameter values close to those measured by Ryan *et al.*<sup>14</sup> for primary cosmic rays below about  $10^{12}$  eV.

We have reported elsewhere<sup>33</sup> that the primary cosmic-ray intensity obtained from this analysis of underground muon events is lower than the intensity obtained by several analyses of extensive air-shower electron-number measurements. We plan to investigate this discrepancy further. The lateral structure of muon showers is important for the rates of multiple-muon events in a detector of limited area. A previous analysis by Adcock *et al.*<sup>34</sup> of decoherence data obtained from the University of Utah muon detector<sup>35</sup> found that an average  $p_T$  value of  $0.60 \pm 0.05$  GeV/c was required for the meson parents of the muons. A different interaction model was used in that calculation than was used in the work reported here. However, their conclusion may indicate that a scaling model with an energy-independent transverse-momentum distribution determined at accelerator energies will not be successful in describing the distribution of separations of muon pairs. A study of the experimental decoherence curve and its implications is now in progress.

*Note added in proof.* Since the completion of this paper, final results have been obtained for muon decoherence measurements, using the main Utah

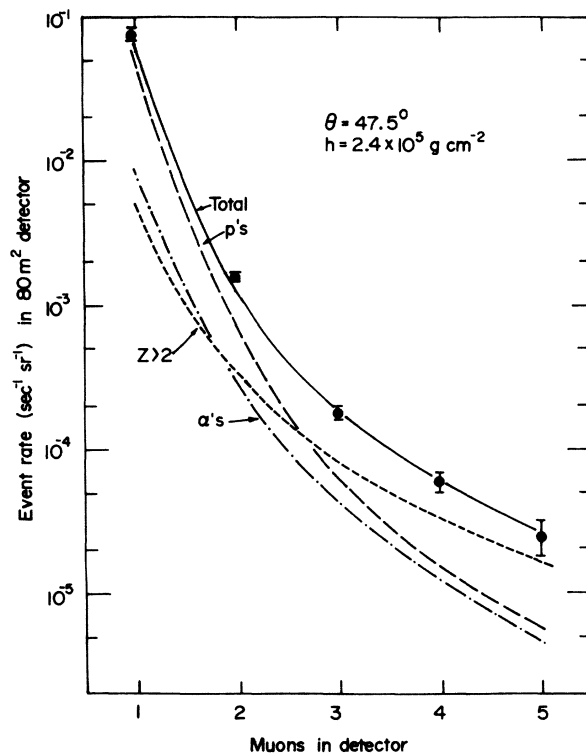


FIG. 6. Predicted rates of events of multiplicity 1-5 produced by the various primary cosmic-ray constituents.

detector and auxiliary detectors. These depend on the lateral structure of muon showers to distances greater than 60 m. A comparison with the decoherence curve predictions of our model indicates a need for broadening the pion transverse momentum distribution beyond the one used, which had  $\langle p_T \rangle = 0.38$  GeV/c for pions with  $x > 0.01$ . In order to preserve agreement with the multiple-muon-event rates in the detector, we expect more high-energy primary cosmic rays to be required, in better agreement with extensive air-shower data.

## ACKNOWLEDGMENTS

We are grateful for discussions with W. V. Jones concerning the breakup of heavy nuclei in nucleus-nucleus collisions. We also gratefully acknowledge the assistance of R. L. Spencer with calculations of the high-multiplicity predictions.

\*Research supported by the National Science Foundation.

†Deceased

<sup>1</sup>R. P. Feynman, Phys. Rev. Lett. **23**, 1415 (1969).

<sup>2</sup>J. Benecke, T. T. Chou, C. N. Yang, and E. Yen, Phys. Rev. **188**, 2159 (1969).

<sup>3</sup>G. H. Lowe, M. O. Larson, H. E. Bergeson, J. W. Cardon, J. W. Keuffel, and J. West, preceding paper Phys. Rev. D **12**, 651 (1975).

<sup>4</sup>J. W. Elbert and G. W. Mason, Univ. of Utah Internal Report No. UUCR 122, 1974 (unpublished).

- <sup>5</sup>J. V. Allaby *et al.*, CERN Report No. 70-12, 1970 (unpublished).
- <sup>6</sup>H. Bøggild, K. H. Hansen, and K. Suk, Nucl. Phys. **B27**, 1 (1971).
- <sup>7</sup>R. Hagedorn, Nuovo Cimento **52A**, 1336 (1967).
- <sup>8</sup>M. Antinucci, A. Bertin, P. Capiluppi, M. D'Agostino-Bruno, A. M. Rossi, G. Vanini, G. Giacomelli, and A. Bussiere, Nuovo Cimento Lett. **6**, 121 (1973).
- <sup>9</sup>D. R. O. Morrison, CERN Report No. CERN/D.Ph. II/PHYS. 72-19, 1972 (unpublished). Besides being the basis for our  $\bar{p}$  assumptions, this report gave data which were used as a basis for our parametrization of the "seagull effect" for pions. Figure 11.4 of the report was used to obtain the factor  $\exp[-p_T/(0.141 + 0.172x - 0.172x^2)]$  for pions which replaced  $\exp[-p_T/(A_6 + A_7|x|)]$  in Eq. (1). The change was small in the  $x$  region in which the original fits were made.
- <sup>10</sup>P. Slattery, Phys. Rev. Lett. **29**, 1624 (1972).
- <sup>11</sup>Z. Koba, H. B. Nielsen, and P. Olesen, Nucl. Phys. **B40**, 317 (1972).
- <sup>12</sup>J. W. Elbert, A. R. Erwin, and W. D. Walker, Phys. Rev. D **3**, 2042 (1971).
- <sup>13</sup>T. K. Gaisser and G. B. Yodh, in *Proceedings of the Thirteenth International Cosmic Ray Conference* (University of Denver, Denver, 1973), Vol. 3, p. 2140.
- <sup>14</sup>M. J. Ryan, J. F. Ormes, and V. K. Balasubrahmanyam, Phys. Rev. Lett. **28**, 985 (1972).
- <sup>15</sup>B. G. Cartwright, M. Garcia-Munoz, and J. A. Simpson, in *Proceedings of the Twelfth International Conference on Cosmic Rays* (University of Tasmania, Hobart, 1971), Vol. 1, p. 215.
- <sup>16</sup>M. Shapiro and R. Silberberg, Annu. Rev. Nucl. Sci. **20**, 323 (1970).
- <sup>17</sup>V. K. Balasubrahmanyam and J. F. Ormes, Astrophys. J. **186**, 109 (1973).
- <sup>18</sup>G. Faeldt, H. Pilkuhn, and H. B. Schlaile, University of Karlsruhe Report No. TKP 24/72, 1972 (unpublished).
- <sup>19</sup>F. A. Berry, E. Bollay, and N. Beers, *Handbook of Meteorology* (McGraw-Hill, New York, 1945).
- <sup>20</sup>J. L. Osborne, Ph.D. thesis, University of Durham, 1966 (unpublished).
- <sup>21</sup>G. W. Carlson, Ph.D. thesis, University of Utah, 1973 (unpublished).
- <sup>22</sup>G. Carlson and J. L. Morrison, Univ. of Utah Internal Report No. UUCR 118 (1974).
- <sup>23</sup>A. A. Petrukhin and V. V. Shestakov, Can. J. Phys. **46**, S377 (1968).
- <sup>24</sup>R. P. Kokoulin and A. A. Petrukhin, in *Proceedings of the Twelfth International Conference on Cosmic Rays* (University of Tasmania, Hobart, 1971), Vol. 4, p. 2436.
- <sup>25</sup>G. L. Cassiday, Phys. Rev. D **3**, 1109 (1971).
- <sup>26</sup>A. G. Wright, J. Phys. A **7**, 2085 (1974).
- <sup>27</sup>S. Miyake, in *Proceedings of the Thirteenth International Cosmic Ray Conference* (University of Denver, Denver, 1973), Vol. 5, p. 3638.
- <sup>28</sup>A. Bassetto and J. Dias de Deus, Nuovo Cimento Lett. **9**, 525 (1974).
- <sup>29</sup>The discrepancy mentioned in the text occurred in a report but was removed in the published paper [J. Engler *et al.*, Nucl. Phys. **B84**, 70 (1974)].
- <sup>30</sup>J. Engler, W. Flauger, B. Gibbard, F. Mönning, K. Pack, K. Runge, and H. Schopper, Nucl. Phys. **B46**, 173 (1973).
- <sup>31</sup>G. B. Yodh, Y. Pal, and J. S. Trefil, Phys. Rev. Lett. **28**, 1005 (1972).
- <sup>32</sup>Very recently we have received two reports from the University of Durham and the University of Lodz: Amr Goned, Univ. of Durham report (unpublished); A. Goned, T. R. Stewart, A. W. Wolfendale, and J. Wdowczyk, Univ. of Lodz report (unpublished). In the work described in these papers, an independent calculation of the predictions of scaling for multiple-muon rates in the Utah underground muon detector was done. These authors used different parametrizations of the inclusive particle distributions and the assumptions differed in many details from ours. Since they did not use the Monte Carlo technique, some effects of fluctuations in the development of hadronic showers are neglected in their calculation. Nevertheless, the conclusions concerning scaling and the primary cosmic-ray spectra and composition obtained from the muon data agree with ours. We feel these results indicate that the results of these calculations are not very sensitive to small perturbations of the input assumptions.
- <sup>33</sup>J. W. Elbert, M. O. Larson, G. H. Lowe, J. L. Morrison, G. W. Mason, and R. L. Spencer, J. Phys. A **8**, L13 (1975).
- <sup>34</sup>C. Adcock, R. B. Coats, A. W. Wolfendale, and J. Wdowczyk, J. Phys. A **3**, 697 (1970).
- <sup>35</sup>R. B. Coats, S. Ozaki, R. O. Stenerson, H. E. Bergeson, J. W. Keuffel, M. O. Larsen, G. H. Lowe, J. L. Osborne, and J. H. Parker, J. Phys. A **3**, 689 (1970).